A Transverse Polarimeter for a Linear Collider of 250 GeV $e^{\pm}$ Beam Energy

Itai Ben Mordechai[1] **and Gideon Alexander**[2]

School of Physics and Astronomy
Raymond and Beverly Sackler Faculty of Exact Sciences
Tel-Aviv University, 69978 Tel-Aviv, Israel

Abstract

The setup and features of a transverse polarimeter based on Compton scattering is described for a 250 GeV electron (positron) beam and its performance is investigated via a Monte Carlo data sample. The position of the Compton backward scattered electrons are registered by a Silicon pixel detector situated some 38 meters away from the $e\gamma$ collision position. Specifically it is shown that, for the planned International Linear Collider beam parameters at 250 GeV, a measurement of the transverse polarization reaches a statistical precision of $\leq 0.5\%$ within a very short time. The over all systematic error is estimated to be $\sim 0.2\%$.

July 30, 2012

[1]Email: *itaibm@gmail.com*
[2]Email: *gideona@post.tau.ac.il*

1 Introduction

In planning future high energy e^+e^- linear colliders, like the International Linear Collider (ILC) and the Compact Linear Collider (CLIC), the benefit of the implementation of a longitudinal polarized $e^{\pm}$ beams has been stressed in many studies [1]. Although even if only the electron beam is longitudinal polarized the collider physics capabilities is increased, as has been demonstrated with the SLC, the situation where both beams are polarized allows additional physics problems to be investigated.

More recently the benefit from the investigation of e^+e^- interactions with transversed polarized beams has also been emphasized [2]. Unlike the case of the longitudinal polarization in the transverse polarization case both the electron and the positron beams have to be polarized in order to benefit from it. To utilize the transverse polarized colliding beams it is necessary to have measuring devices that can measure the transverse polarization values, near or at the e^+e^- interaction point ($IP_{e^+e^-}$), down to a level of 0.5% or even better.

At low electron beam energies transverse polarization measurement devices, denoted by Transverse Polarimeters (TPOL), have been designed constructed and operated successfully [3]. In the present work we study the feasibility to design and construct a transverse polarimeter at high beam energy of 250 GeV, envisaged for the ILC, having a precision of $\leq 0.5\%$ via the Compton scattering of a polarized laser light off the $e^{\pm}$ beams.

2 The Compton scattering

For the basic formulae of the Compton scattering of a laser beam on an electron beam we have followed closely reference [3]. In the electron center of mass (CM) system (see Fig. 1) the differential Compton scattering is given by

$$\frac{d\sigma}{d\Omega}(S,P) = \Sigma_0 + S_1\Sigma_1 + S_3[P_y\Sigma_{2y} + P_z\Sigma_{2z}] \tag{1}$$

where

$$\begin{aligned}
\Sigma_0 &= C[(1+\cos^2\theta) + (k_i - k_f)(1-\cos\theta)] \\
\Sigma_1 &= C\cos(2\phi)\sin^2\theta) \\
\Sigma_{2y} &= -Ck_f\sin\phi\sin\theta(1-\cos\theta) \\
\Sigma_{2z} &= -C(1-\cos\theta)(k_f+k_i)\cos\theta
\end{aligned}$$

Here $P = (P_x, P_y, P_z)$ is the polarization of the initial electron in Cartesian coordinates. S_1 is the linear polarization component of the photon and S_3 is the circular component of the photon. The initial and final photon momenta k_i and k_f are defined in the electron CM system and $C = 0.5r_0^2k_f^2/k_i^2$ where r_0 is the classical radius of the electron. The angles θ and ϕ

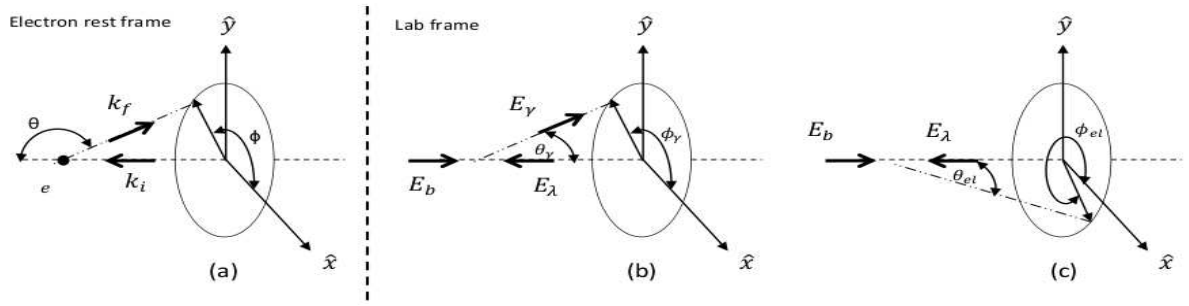

Figure 1: Geometry and coordinate system of the Compton scattering, showing in (a) the incoming electron rest frame and in (b) in the laboratory system both for the back scattering angles of the photon. In (c) the process is shown in the laboratory system for the scattered electron.

are the polar and azimuthal angles of the backward scattered photon in the electron CM system. To transform these formulae to the laboratory system one has the relations

$$\cos\theta = \frac{E_{beam} - E_\gamma(1 + 1/k_i)}{E_{beam} - E_\gamma} \quad \text{and} \quad \mathrm{E}_\gamma = \mathrm{E}_{\mathrm{beam}} + \mathrm{E}_\lambda - \mathrm{E}_\mathrm{e} \tag{2}$$

where the energies are defined in the laboratory system and E_e is the energy of the scattered electron. The electron scattered angle in the laboratory system is given by

$$\theta_e^{lab} = \frac{Y}{1-Y}\frac{m_e}{E_{beam}}\sqrt{\frac{2k_i}{Y} - (2k_i + 1)} \tag{3}$$

where $Y = 1 - E_e/E_{beam}$. The method for the determination of the electron transverse polarization involves the measurement of the y distribution of the scattered electrons on the detector surface which is placed perpendicular to the beam direction. In term of the scattered polar and azimuthal angles y is equal to

$$y = D\sin\phi\tan\theta_e^{lab} \quad \overset{\theta_e^{lab} \ll 1}{\longrightarrow} D\sin\phi\theta_e^{lab} \tag{4}$$

where D is the distance between the Compton interaction point and the detector surface. In practice one considers $< y >$, the average value of the measured y positions.

3 Transverse Polarimetry for the ILC

In our study we consider the case where the laser beam has no linear component and the electron beam has no longitudinal polarization component. In this case the differential Compton scattering expression given by Eq. 1 reduces to

$$\frac{d\sigma}{d\Omega}(S, P) = \Sigma_0 + S_3 P_y \Sigma_{2y} \tag{5}$$

where the relevant parameters of the ILC are: $S_1 = 0$, $S_3 = \pm 1$, $P_z = 0$, $E_{beam} = 250$ GeV and $D = 37.95$ m [8]. For the polarimeter we have taken a green laser of 2.33 eV. For a given E_e

value the average y is given by;

$$\langle y \rangle \ = \frac{\int \frac{d^2\sigma}{dE_e d\phi} y d\phi}{\int \frac{d^2\sigma}{dE_e d\phi} d\phi} \tag{6}$$

The distribution of $\langle y \rangle$ as a function of E_e for $P_T = 1.0$ and $S_3 = +1$ is shown in Fig. 2.

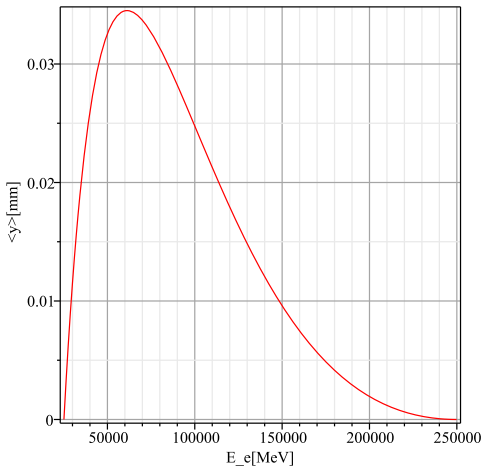

Figure 2: The $\langle y \rangle$ distribution as function of the scattered electron energy for the ILC setup with $P_T = 100\%$, $S_3 = +1$, $\lambda = 2.33$ eV and $D = 37.95$ m.

In order not to be dependent on the exact y position of the $IP_{\gamma e}$ it is a safer way to determine the polarization via the measurement of the difference in $\langle y \rangle$ between the left and right helicity states of the laser ($S = \pm 1$), i.e.

$$\frac{\langle y \rangle_{\ S_3=+1} - \langle y \rangle_{\ S_3=-1}}{2} = P_T \Pi(E_e) \tag{7}$$

where P_T is the transverse polarization level and $\Pi(E_e)$, the Analyzing Power (AP) of the polarimeter, is its value for a 100% polarization. In this way one assures that the measured effect is indeed due to a vertical electron polarization and is not due to an instrumental deficiency.

4 The γe Luminosity

4.1 Luminosity for a continuous laser

The luminosity $\mathcal{L}$ of a continuous laser colliding with a round pulsed electron beam, that is $\sigma_x = \sigma_y = \sigma$, can be expressed [4] as:

$$\mathcal{L} \ = \ \frac{1 + \cos\theta_0}{\sqrt{2\pi}} \frac{I_e}{e} \frac{W_L \lambda}{hc^2} \frac{1}{\sqrt{\sigma_e^2 + \sigma_\gamma^2}} \frac{1}{\sin\theta_0}, \tag{8}$$

where θ_0 is the crossing angle of the two beams, I_e is the mean electron current, W_L is the power of the laser, λ is the wavelength of the laser and σ_e and σ_γ are the rms beam sizes. As

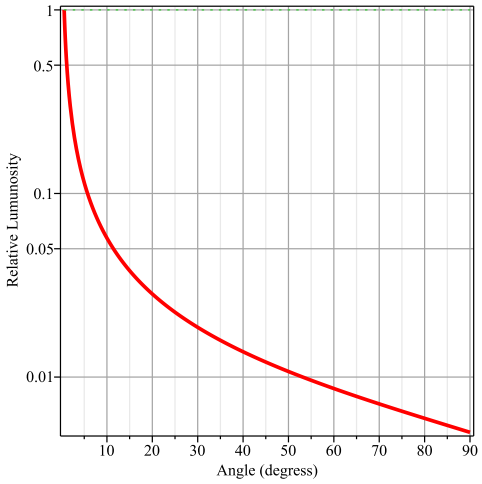

Figure 3: The relative $e\gamma$ luminosity as a function of the crossing angle θ_0 of the incident electron and laser beams.

expected, the luminosity will decrease substantially when the angle between the laser and the beam will approach 90^o (see in Fig. 3) so that a continuous laser beam perpendicular to the electron beam will result in an undesired very low luminosity[3]. For a small crossing angle θ_0 one has:

$$\mathcal{L} \;=\; 8.36\ 10^{24} cm^{-2} s^{-1}\ \frac{\lambda}{\sqrt{\sigma_e^2+\sigma_\gamma^2}}\frac{I_e W_L}{\theta_0}\ . \tag{9}$$

According to Ref. [5] at the ILC where $\sigma_e \ll \sigma_\gamma$, and with the following parameters settings:
$\theta_0 = 0.01$ rad,
$\lambda = 532$ nm $= 2.33$ eV,
$\sigma_\gamma = 50\ \mu$m,
$W_L = 0.5$ W,
$I_e = 9\ \mu$A,
one obtains a luminosity of

$$\mathcal{L}(\gamma e) \;=\; 1.75\times 10^{29}\ cm^{-2}s^{-1}\ . \tag{10}$$

4.2 The luminosity value with a pulsed laser

For a pulsed laser the γe luminosity is given by [6]:

$$\mathcal{L} \;=\; f_b N_e N_\gamma g \tag{11}$$

where f_b is the number of bunch crossing per second, N_e the number of electrons per bunch, N_γ the number of photons per laser pulse and g is a geometrical factor which takes in account the spatial overlap of the two beams. For a small crossing angle θ_0 one has:

$$g^{-1} \;=\; 2\pi\sqrt{\sigma_{xe}^2+\sigma_{x\gamma}^2}\sqrt{(\sigma_{ye}^2+\sigma_{y\gamma}^2)cos^2(\theta_0/2)+(\sigma_{ze}^2+\sigma_{z\gamma}^2)sin^2(\theta_0/2)}\ . \tag{12}$$

[3]Note that $\theta_0 = 0^o$ means here that the laser and the beam directions are exactly opposite.

If the transverse dimensions of the electron beam are small in comparison to the laser focus i.e., $\sigma_{xe} \ll \sigma_{x\gamma}$ and $\sigma_{ye} \ll \sigma_{y\gamma}$ (which certainly is valid at the $IP_{\gamma e}$ region), one obtains for g^{-1} :

$$g^{-1} \;=\; 2\pi\sigma_{x\gamma}\sigma_{y\gamma}\sqrt{1+(0.5\theta_0\sigma_{z\gamma}/\sigma_{y\gamma})^2} \tag{13}$$

and for the luminosity:

$$\mathcal{L} \;=\; \frac{f_b N_e N_\gamma}{2\pi\sigma_{x\gamma}\sigma_{y\gamma}\sqrt{1+(0.5\theta_0\sigma_{z\gamma}/\sigma_{y\gamma})^2}} \;=\; \frac{\mathcal{L}_{max}}{\sqrt{1+(0.5\theta_0\sigma_{z\gamma}/\sigma_{y\gamma})^2}} \tag{14}$$

where $\mathcal{L}_{max}$ is the maximum luminosity reached at very small θ_0 angle for a given transverse size $\sigma_{x\gamma}\sigma_{y\gamma}$, namely:

$$\mathcal{L}_{max} \;=\; \frac{f_b N_e N_\gamma}{2\pi\sigma_{x\gamma}\sigma_{y\gamma}}\,. \tag{15}$$

Note that this last formula is very similar to the expression given for the luminosity of e^+e^- colliding beams. In the ILC, the dimensions of the electron bunches at $IP_{e^+e^-}$ are smaller than that of the laser. The number of bunches per second is $f_b = 14100$ and each bunch consists of $N_e = 2\times10^{10}$ electrons. From this follows that the $e\gamma$ luminosity at the $IP_{\gamma e}$ is

$$\mathcal{L}_{max}(IP_{\gamma e}) \;=\; 4.49\times\frac{N_\gamma}{\sigma_{x\gamma}\sigma_{y\gamma}}\;10^{13}cm^{-2}s^{-1} \tag{16}$$

where N_γ is the number of laser photons per pulse and the laser is fired in synchronization with the same pulse repetition rate as the accelerator. For a round laser focus with $\sigma_{x\gamma} = \sigma_{y\gamma} = 50\mu m$ one obtains:

$$\mathcal{L}_{max}(IP_{\gamma e}) \;=\; 1.12\times\frac{j_\gamma[\mu J]}{\epsilon_\gamma[eV]}10^{31}cm^{-2}s^{-1} \tag{17}$$

where j_γ and ϵ_γ are the laser current and energy. The Compton $e\gamma$ luminosity at the ILC operating at 0.25 TeV beam energy for three pulsed laser configurations are shown in Table 1.

Table 1: Compton $e\gamma$ luminosity before the $IP_{e^+e^-}$ of the ILC operating at 0.25 TeV beam energy with a round pulsed laser of $\sigma_{x\gamma} = \sigma_{y\gamma} = 50\mu m$. A full synchronization between the beam bunches and the laser repetition is assumed.

ϵ_γ (eV)	λ (nm)	$< W_L >$ (Watt)	j_γ (μJ)	$\mathcal{L}_{max}$ (10^{31}cm$^{-2}s^{-1}$)
1.165	1064	1	71	68.3
2.33	532	0.5	35	16.8
4.66	266	0.2	14	3.4

5 The polarimeter setup

A sketch of the Compton scattering collision setup is shown in Fig. 4. The 250 GeV electron beam is moving in the $+z$ direction reaching the first two $B_1(-y)$ and $B_2(+y)$ magnets which steer the beam to a parallel straight trajectory. In position 2 the laser beam collides with the electron beam. The unperturbed beam is then restored to its original trajectory by the set of the $B_2(+y)$ and $B_1(-y)$ magnets all of which have a strength of 0.097 T. The scattered electrons which suffered a loss of energy will be separated in the x direction according to their energy values to reach the detector at a distance of 37.95 m.

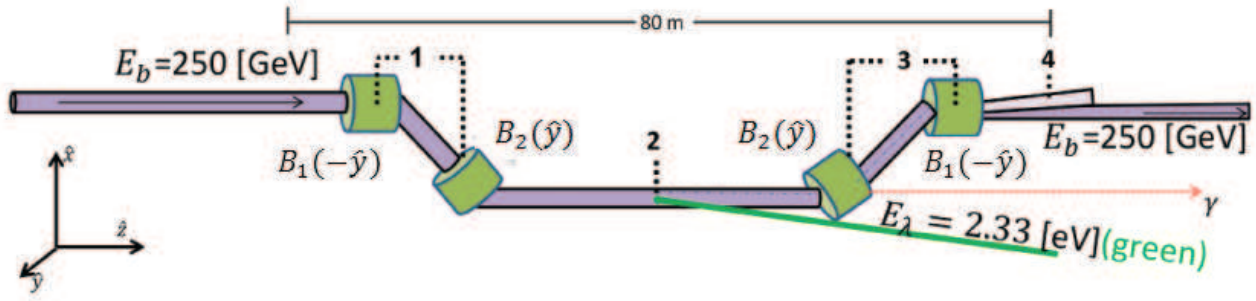

Figure 4: The setup scheme of the laser collision with the 250 GeV electron beam which moves in the z direction. The magnets are steering the beam to a parallel trajectory for the laser collision point and back to their original direction. The scattered electrons are deviated from the bean direction toward a detector 37.95 m away.

5.1 The energy spectrometer

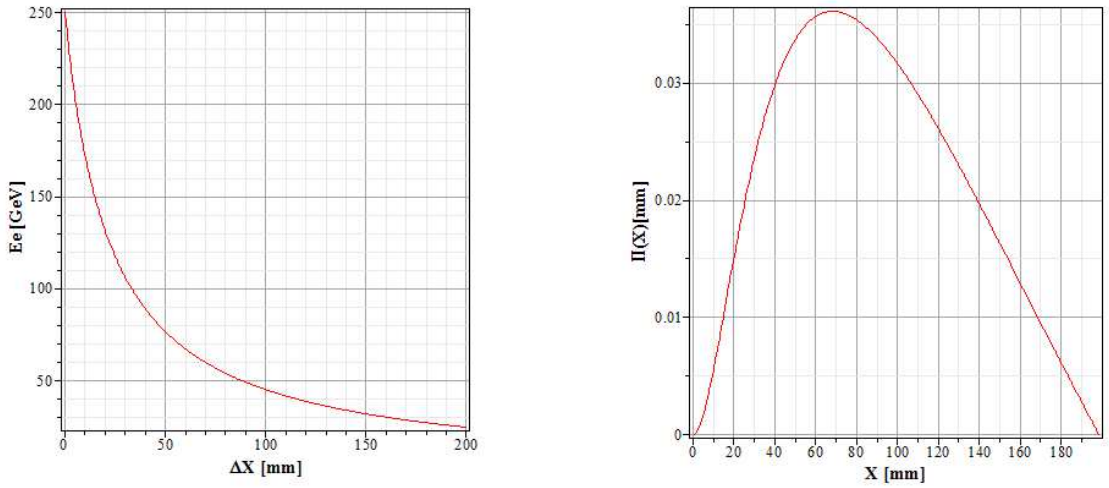

Figure 5: Left: The scattered electron energy as a function of the x shift from the non-scattered beam. Right: The transverse polarization analyzing power $\Pi(x)$ as a function of the x shift.

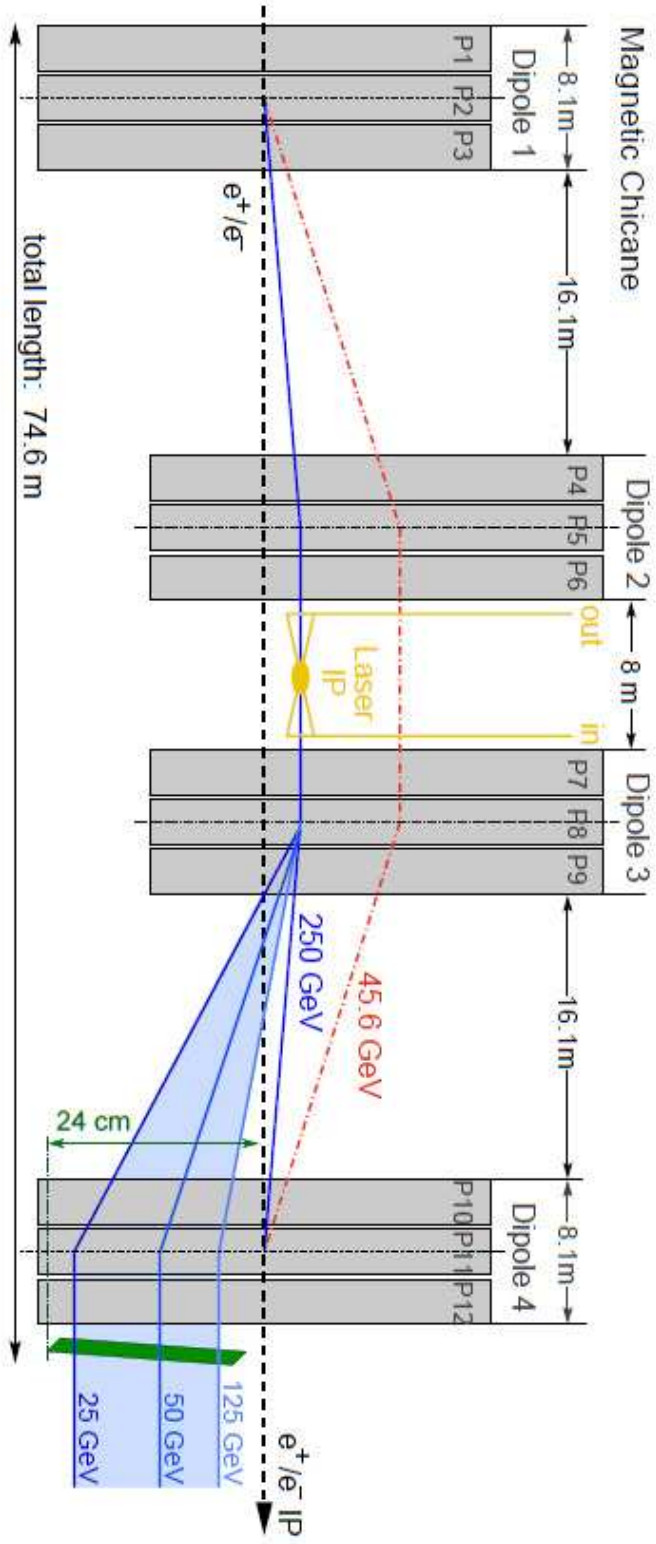

Figure 6: The general scheme of the envisaged ILC of the four magnets chicane for the Compton polarimetry taken from Ref. [8]. The shifted electron beam shown by the solid line is colliding with the laser beam and then restored to its original trajectory (dashed line). The scattered electrons are separated according to their energy values. The 45.6 GeV beam (dot dashed line) is planned to be used for calibration purposes.

The relation between x and the energy of the scattered electrons is shown in Fig. 5(left) was determined from a Monte Carlo (MC) program [7] using the actual general scheme of the envisaged ILC four magnets chicane [8] as shown in Fig. 6. A fit to the distribution shown in Fig. 5(left) yields

$$E_e = \frac{10^6}{4 + 18.04 \cdot x[mm]} \text{ MeV} . \tag{18}$$

By replacing the energy dependence in Eq. 7 by its dependence on x according to Eq. 18 one obtains the dependence of AP on x. As can be seen from in Fig. 5(right), the AP changes considerably with x and reaches its maximum value around 70 mm from the main beam direction.

5.2 The detector

For the detection of the scattered electrons we consider only a position measurement using a Silicon pixel detector placed at a distance of 37.95 m from the Compton $IP_{\gamma e}$. The active dimension of the detector is 2×200 mm^2. The size of the pixels cell taken is 50 × 400 μm^2 similar to the one used in the ATLAS detector [9]. This scheme yields an approximate two dimensional resolution of 14.4× 115.5 $m\mu^2$ [10] with a data read-out rate of 160 Mb/sec.

For the simulation and analysis of the polarization measurement we have used a Monte Carlo program which generates the Compton scattering and simulates the polarimeter setup [7].

6 The polarization measurement

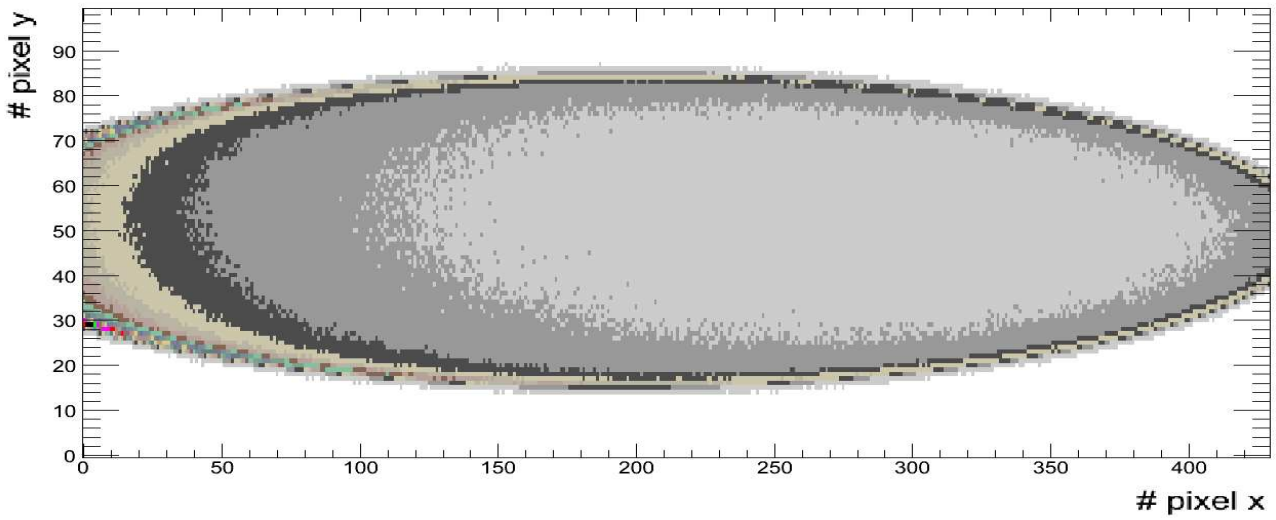

Figure 7: A MC ILC simulated pixel detector image, in arbitrary units, after it was hit for 1 sec by the Compton scattered electrons for $S_3 = +1$ and $P_T = 0.9$.

6.1 The measurement method

For the measurement of the polarization we have used the scattered electron detector hits in the left and right ($S_3 = +1$ and $S_3 = -1$) helicity positions of the laser. A 1 second typical hit distribution of the detector is shown in Fig. 7 for $S_3 = +1$ and $P_T = 0.9$. After the readout of the pixel detector's x and y positions of the hits we calculate the average $\langle y \rangle$ as a function of x sampled in 2 mm steps for the two laser helicity states. In Fig, 8(left) the y distribution for $S_3 = +1$ is shown in the range of 36 $mm \leq x \leq 38$ mm where a clear asymmetry due to the transverse polarization is seen.

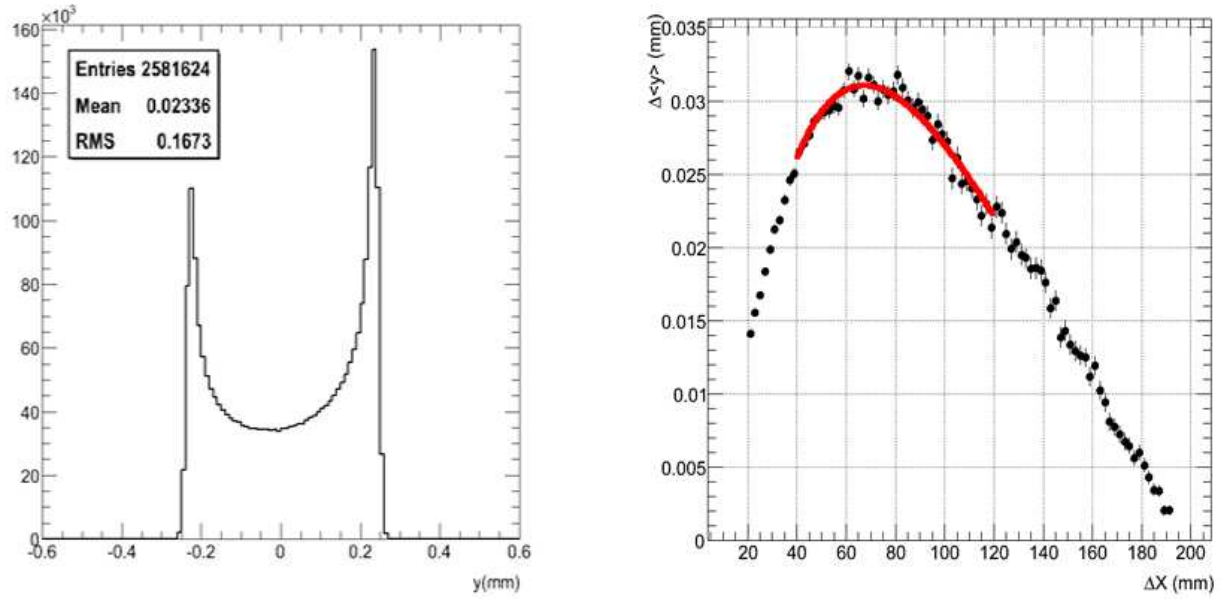

Figure 8: Monte Carlo data simulation. Left: The distribution of y within the x range of 36 to 38 mm from the electron beam direction for the $S_3 = +1$ helicity and $P_T = 0.9$. A clear asymmetry due to the transverse polarization is seen. Right: The dependence of $P_T\Pi(x)$ on x reevaluated in steps of 2 mm obtained from 1 sec run. The solid line is the results of a fit of Eq. 19 to the Monte Carlo data.

We next calculate the quantity $(\langle y \rangle_L - \langle y \rangle_R)/2$ as a function of x. The results for 1 sec run (14100 bunches) are shown in Fig. 8(right) where the small fluctuations of the MC data points are due to the finite beam dimension and the pixel detector resolution. Next we fit P_T from the MC data in a given x range around its maximum value according to Eq. 19

$$\Delta y(x) = \left. \frac{\langle y \rangle_L - \langle y \rangle_R}{2} \right|_X = P_T \Pi(x) \tag{19}$$

where $\Pi(x)$ is the analyzing power. The result of the fit, shown by the solid line in Fig. 8(right), yielded $P_T = 0.899 \pm 0.003$, with χ^2/dof =1.39, which agrees very well with the MC input value of $P_T = 0.9$.

6.2 The statistical error

We have evaluated the statistical error on the transverse polarizations measurements from our Monte Carlo data sample assuming a zero detector dead time. Obviously this error is related to the number of scattered electrons recorded by the detector. This is shown in Fig. 9 where the error dependence on the measurement time can be expressed by $\Delta P_T/P_T = 0.29 \times t^{-0.53}$ %. As expected, already for a very short measurement time, the statistical error can be neglected in comparison with the systematic errors which are discussed in the following section.

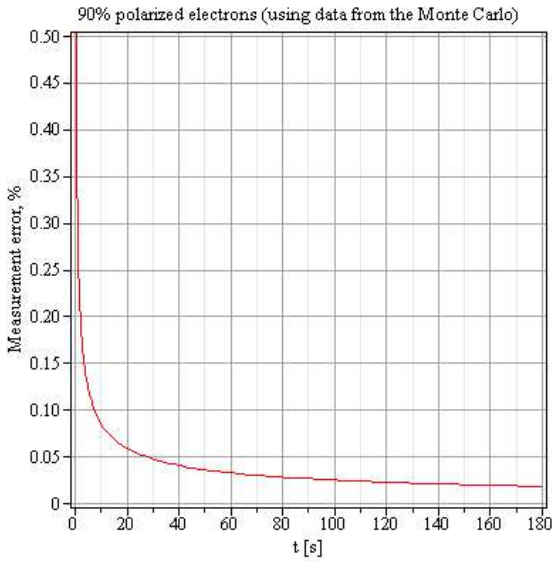

Figure 9: The measurement statistical error on a $P_T = 0.9$ level as a function of the measuring time derived from the Monte Carlo data sample assuming zero detector dead time.

6.3 The systematic errors

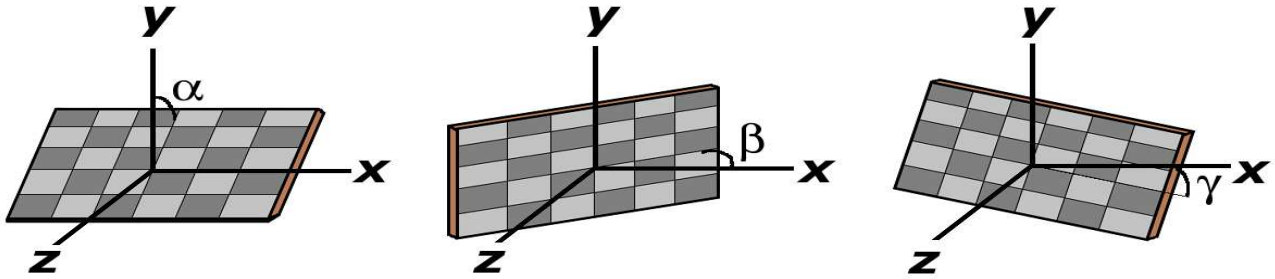

Figure 10: The deviation of the Silicon pixel detector orientation which is set to be perpendicular to the non-scattered electron beam that moves in the z direction.

A substantial contribution to the systematic error of the polarization measurement is coming from possible y displacement of the $IP_{\gamma e}$ and or the pixel detector. Due to the fact that the

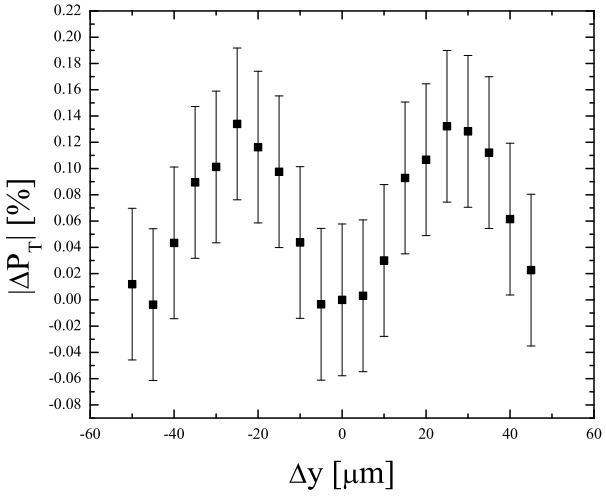

Figure 11: The ΔP_T dependence on Δy calculated for $P_T = 0.9$ via a MC program. The statistical errors correspond to a measurement time of 1 minute with the ILC and polarimeter setup as described in the text.

dimension of the pixels are finite, in our setup of 50 μm in the y direction, one does not achieve a complete Δy compensation via Eq. 7. From our MC simulation we obtain a quasi-sinusoidal dependence of ΔP_T on Δy which is shown in Fig. 11. As expected a maximum compensation of the Δy displacement is reached when its value is $n \times 50$ μm where $|n|$ is equal to zero or an integer. At the same time the systematic error on $|P_T|$ does not exceed the value of $\sim 0.13\%$. This systematic error and other ones have been estimated by changing individually various parameters of the planned ILC and its polarimeter setup according to their uncertainties estimated in Ref. [5]. These are listed in Table 2. The first three parameters of the table concern the displacements of the $IP_{\gamma e}$ or the pixel detector positions. The next three parameters are associated with detector orientation with respect to the beam position as defined in Fig. 10. The next two parameters are related to the magnetic field of the spectrometer. The following pair of parameters are connected to the beam tremor and the last two parameters are related to the beam energy uncertainty. As seen from the table, the over all systematic error added in quadrature amounts to 0.20 % . Additional sources of systematic error like those related to the radiation background from the collider and the polarimeter structure will have to be evaluated after their detailed design and construction.

Acknowledgments

We would like to thank S. Riemann and many of her colleagues in the Linear Collider groups of DESY/Zeuthen and DESY/Hamburg for their many useful comments and suggestions. Our thanks are in particular due to J. List for allowing us to make use of her Monte Carlo

Table 2: A list of the collider and polarimeter setup parameters that are expected to contribute to the systematic errors of the transverse polarization measurement. From the assessed systematic uncertainties of these parameters the corresponding systematic errors were obtained from a MC program simulating the ILC polarimeter features with a beam polarization value of $P_T = 0.9$.

Source of the systematic error	Δ	$\lvert\Delta P_T\rvert$ %
Δy axis displacement	≥ 25 μm	0.13
Δx axis displacement	0.1 mm	0.007
Δz axis displacement	1 cm	0.08
$\Delta\alpha$ deviation of the detector	0.1^0	0.002
$\Delta\beta$ deviation of the detector	0.1^0	0.004
$\Delta\gamma$ deviation of the detector	0.1^0	0.1
Spectrometer ΔB_1	0.0001 T	0.02
Spectrometer ΔB_2	0.0001 T	0.005
y axis beam position tremor	5 μm	0.01
x axis beam position tremor	5 μm	0.03
Beam energy tremor	0.22 GeV	0.03
ΔE_{beam} beam energy	0.22 GeV	0.052
$\sqrt{\sum_i \Delta P_i^2}$	0.20%	

program and her help in its adaptation to out transverse polarimeter setup.

References

[1] See e.g. G. Moortgat-Pick et al., Phys. Rept. 460 (2008) 131.

[2] See e.g. T.G. Rizzo, SLAC-PUB-14280, *arXiv:1011.2185*; K. Desch, LC-PHSM-2003-002; F. Franco-Sollova, LC-PHSM-2004-011.

[3] See e.g. D.P. Barber et al., Nucl. Inst. and Method. A329 (1993) 79 for more details.

[4] G. Bardin, et al., *Compton polarimeter studies for TESLA*, DESY print, TESLA 97-03.

[5] J. Brau (Ed), *et al.,* ILC collaboration, arXiv:0712.1950 [physics.acc-ph].

[6] T. Suzuki, *General formulae of luminosity for various types of colliding beam machines*, KEK-76-3 (1976), *http://ccdb4fs.kek.jp/cgi-bin/img_index?197624003* .

[7] C. Bartels et al., Nucl. Inst. Meth. A623 (2010) 570.

[8] S. Boogert et al., JINST 4 (2009) P10015.

[9] ATLAS pixel collaboration, Technical Design Report, (CERN/LHCC, 98-13), 2007.

[10] L. Rossi et al., *Pixel detectors: from fundamentals to applications* Springer Verlag, 2006.